The physiological response of Saccharomyces cerevisiae to temperature stress

Postmus, J.

Publication date
2011

CHAPTER 4

DYNAMIC REGULATION OF MITOCHONDRIAL RESPIRATORY CHAIN EFFICIENCY IN *SACCHAROMYCES CEREVISIAE*

DYNAMIC REGULATION OF MITOCHONDRIAL RESPIRATORY CHAIN EFFICIENCY IN *SACCHAROMYCES CEREVISIAE*

Jarne Postmus[1], Işil Tuzun[2], Martijn Bekker[2], Wally H. Müller[3], M. Joost Teixeira de Mattos[2], Stanley Brul[1] and Gertien J. Smits[1*]

[1] Department of Molecular Biology and Microbial Food Safety, Swammerdam Institute for Life Sciences, University of Amsterdam, Science Park 904, 1098 XH Amsterdam

[2] Department of Molecular Microbial Physiology, Swammerdam Institute for Life Sciences, University of Amsterdam, Science Park 904, 1098 XH Amsterdam

[3] Department of Biology, Biomolecular Imaging, Institute of Biomembranes, Utrecht University, Padualaan 8, 3584 CH Utrecht.

This chapter is in preparation for submission

ABSTRACT

To adapt to changes in the environment, cells have to dynamically alter their phenotype in response to changes in for instance temperature and oxygen availability. Interestingly, mitochondrial function in *Saccharomyces cerevisiae* is inherently temperature sensitive; above 37ºC yeast cells can not grow on respiratory carbon sources. To investigate this phenomenon, we studied the effect of cultivation temperature on the efficiency of the yeast respiratory chain in glucose-limited chemostats. We determined that even although the specific oxygen consumption rate did not change with temperature, oxygen consumption no longer contributed to mitochondrial ATP generation above 37ºC. Remarkably, between 30ºC to 37ºC we observed a linear increase in respiratory efficiency with growth temperature, up to a P/O of 1.4, almost the theoretical maximum that can be reached *in vivo*. The temperature dependent increase in efficiency required the presence of the mitochondrial glycerol-3-phosphate dehydrogenase *GUT2*. Decreased oxygen availability also affected respiratory chain efficiency revealed a strong decrease of the P/O value. Our data show that, even in the absence of alternative oxidases or uncoupling proteins, yeast has retained the ability to dynamically regulate the efficiency of coupling of oxygen consumption to proton translocation in the respiratory chain in response to changes in the environment.

INTRODUCTION

Unicellular organisms have to cope with environmental changes in order to maintain homeostasis and to survive. These changes may perturb cellular functions, such as metabolic fluxes, destabilized cellular structures, chemical gradients, etc., and can thus result in arrest of growth or even cell death. Therefore, microbes, such as yeasts, rapidly adapt to challenging conditions by altering their genetic expression profile or tuning the activity of key enzymes to function in the changes environment [1-5]. Adaptive responses put a significant additional energetic burden on the cells, since the transcription cascade requires a substantial expenditure of energy [6-8]. The fraction of the energy generated in catabolism that is used in processes other than biomass production is the so-called maintenance energy [9]. Increases in maintenance energy may be spent on for instance maintenance of membrane gradients, turnover of (damaged) cell components, or energetically suboptimal biosynthetic pathways [6].

Baker's yeast has multiple strategies for energy generation. Carbohydrates are dissimilated into pyruvate, which is located at a key branching point in carbohydrate metabolism [10]. During fermentative metabolism, pyruvate is converted into acetaldehyde and subsequently reduced to ethanol. In respiratory metabolism pyruvate is converted into acetyl coenzyme A. This acetyl CoA is used to produce NADH in the mitochondria via the tricarboxylic acid cycle. Subsequently, the NADH synthesized is oxidized by the respiratory chain in the mitochondrial membrane, driving proton translocation. The resulting proton motive force is then used to produce ATP (for overview see Figure 4.1).

The amount of NADH oxidized in the electron transport chain to maintain proton motive force or to generate ATP is often larger than expected [11]. Two mechanisms are proposed to underlie this efficiency lowering phenomenon: proton leakage and proton slippage (for review see [12]). Proton leakage can be separated into basal proton leak and regulated proton leakage induced by uncoupling proteins (UCP) [11], while in proton slip the H^+ is never pumped due to a slip in the mechanism of one of the electron driven pumps in the respiratory chain [12]. Incomplete coupling is thought to be important in reducing the production of reactive oxygen species (ROS) [11, 13, 14], in thermogenesis [15] and metabolic regulation [16]. In the plant kingdom, some fungi and protists express alternative oxidases (AOXs). These AOXs couple ubiquinol oxidation to the reduction of water (for review see [17]). The function of such alternative oxidases is thought to be associated with the reduction of ROS formation [18], but may also provide some degree of metabolic flexibility [19]. So far, only the yeast species *Candida parapsilosis* and *Yarrowia lipolytica* have been shown to contain UCP-like proteins [20, 21]. *Yarrowia lipolytica* also contains an AOX, besides its UPCs [22]. The function of UCPs and AOXs in these yeasts is still a matter of debate. For unicellular organisms an active function in thermogenesis is unlikely, since

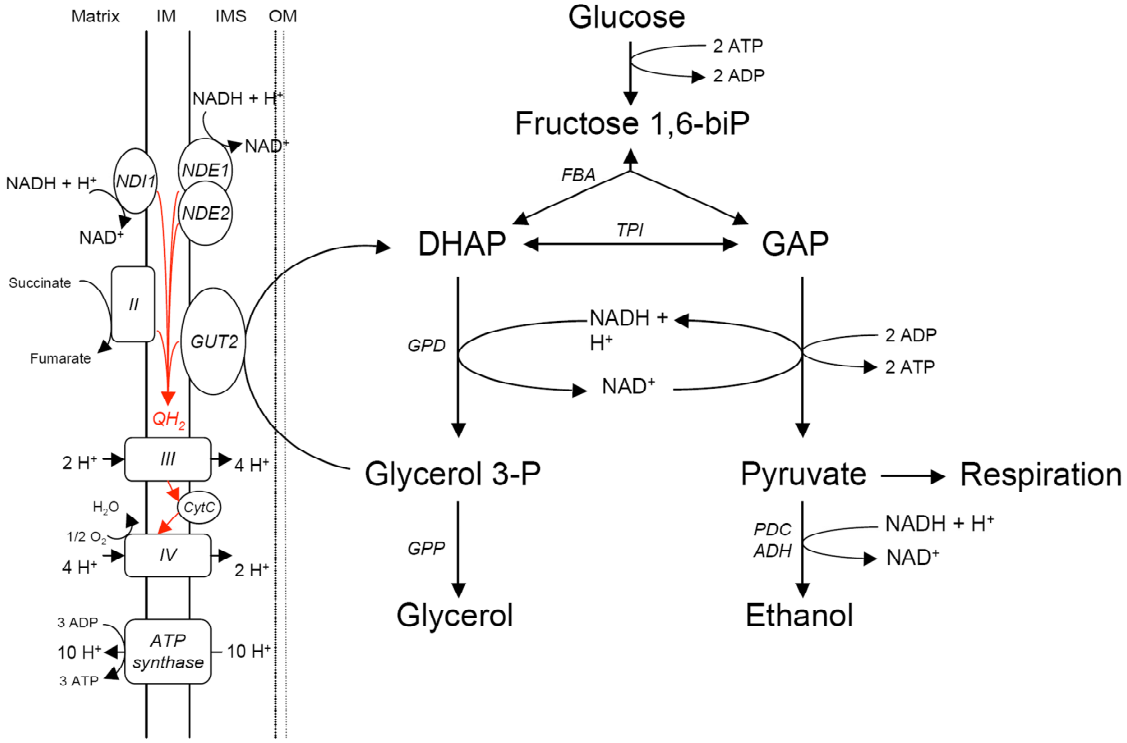

Figure 4.1. Overview of possible mechanisms to couple cytosolic NADH oxidation to the respiratory chain of *S. cerevisiae*. Abbreviations: Nde, external NADH dehydrogenase; Ndi, internal NADH dehydrogenase; Gut2, membrane-bound mitochondrial glycerol-3-phosphate dehydrogenase; II, succinate dyhydrogenase; III, cytochrome bc_1 complex; IV, cytochrome c oxidase.

they cannot maintain a temperature gradient between their interior and the environment [23]. Therefore, the function of these proteins may be in protection against ROS [18] or a role in energy metabolism to function as an electron sink [23], as was shown before for the cytochrome *bd*-II complex in *Escherichia coli* [24]. Since *Saccharomyces cerevisiae* is thought to have a linear respiratory chain [25], no UPCs and no AOXs, adaptation of proton translocation efficiency was not thought possible.

We studied the effect of two common environmental challenges on the regulation of the efficiency of mitochondrial respiratory chain of *Saccharomyces cerevisiae*. We assessed both the effect of changes in the environmental temperature and of lowered oxygen availability. We chose to study the effect of various cultivation temperatures, because in both *E. coli* and yeast, increased temperature was shown to cause an increase in the maintenance energy [7, 26, 27]. In order to sustain growth and simultaneously deal with the increased maintenance, metabolism is expected to be optimized. We found an increased respiratory efficiency with an increase in temperature. Maximal respiratory efficiency was observed at 37ºC and approached the theoretical maximum. Increasing the temperature further resulted in a strong decrease of the efficiency. Challenging the system with respect to oxygen availability resulted in a steep decrease in efficiency at low oxygen levels in the input

gas. For both observations mechanisms are proposed. These data show that, despite the absence of UCPs and AOXs, baker's yeast retains the ability to regulate coupling of oxygen consumption to energy generation in response to environmental change.

MATERIALS AND METHODS

Strains and growth conditions

The yeast strains listed in Table 4.1 were grown in aerobic, carbon-limited 2-liter chemostats (Applikon, Schiedam, The Netherlands) with a working volume of 1 liter at a dilution rate of 0.1 h^{-1}. The medium used for cultivation was based on previously described mineral medium [28] supplemented with 7.5 g l^{-1} glucose. In anaerobic or micro-aerobic cultivations, the medium was supplemented with 10 mg l^{-1} ergosterol and 420 mg l^{-1} Tween, dissolved in absolute ethanol. Final ethanol concentration in the medium was between 10-12 mM. The stirrer speed was set to 800 rpm while the pH was set to pH 5.0 and kept constant by automatic titration with 1M KOH. Stirring rate, pH and temperature were kept constant using an Applikon ADI 1010 Biocontroller (Applikon, Schiedam, the Netherlands). The chemostat was aerated by flushing air at 30 l h^{-1} through the culture. Steady states were verified by off gas analysis for oxygen and carbon dioxide and by dry weight measurements. Pre-cultures were grown overnight in the same mineral medium with 20 g l^{-1} glucose in shake flasks at 30°C and 200 rpm. Plate cultivations were performed on YP plates, containing 1% yeast extract, 2% BactoPepton, 2% BactoAgar and 2% carbon source. The pH was adjusted to 5.0 with 1 M HCl before autoclaving.

Table 4.1. Strains used in this study.

Strain	Genotype	Source
CEN.PK 113-7D	*MATa MAL2-8c SUC2*	Dr. P. Kötter (Frankfurt, Germany)
CEN.PK 113-7A	*MATa MAL2-8c SUC2 his3*	Dr. P. Kötter (Frankfurt, Germany)
JP001	*MATa MAL2-8c SUC2 his3 gut2::HIS3*	This study

Deletion of GUT2

In the CEN.PK background the *GUT2* gene was replaced with *HIS3MX6* cassette via homologous recombination according to Longtine *et al.* [29]. The plasmid pFA6-HisMX6 was used as template DNA for PCR amplification with primers 5'- TGA CCG TGC TAT TGC CAT CAC TGC TAC AAG ACT AAA TAC GTA CTA ATA TA*C GGA TCC CCG GGT TAA TTA A*-3' (the underlined sequence corresponds to 50 nucleotides upstream the *GUT2* ORF) and 5'-ATT ACT CTT GTG AAT GTT ATC TTT GTC ACC CTT AAC TAT CAT GAT CGA TT*G AAT*

TCG AGC TCG TTT AAA C-3' (with the underlined sequence corresponding to 50 nucleotides downstream the *GUT2* ORF). The resulting PCR product was used to transform yeast strain CEN.PK 113-7A. Correct replacement was confirmed by PCR on isolated genomic DNA.

Biomass dry weight measurements

The dry weight concentration was determined in triplicate by filtering 10.0 ml of broth on pre-washed and pre-weighed cellulose acetate membrane filters (pore size 0.45 µm, Schleicher & Schuell MicroSciences, Dassel, Germany). Each filter was washed with 10 ml of demineralized water and dried in a microwave 450W (Whirlpool Promicro 825, Sweden) for 15 min. Filters were cooled in a desiccator and weighed on an electronic analytical balance (Mettler-Toledo AB104, Columbus, Ohio).

Off-gas analysis

The oxygen and carbon dioxide levels in the exhaust gas of the fermentors were monitored on-line using an oxygen analyzer (Servomex Ltd. Paramagnetic O_2 transducer) and a carbon dioxide analyzer (infrared Servomex Xentra 4100 Gas purity Analyser).

Analysis of metabolites

To analyze glucose, ethanol, glycerol, succinate, acetate and trehalose, 1.0 ml of broth was quickly quenched in 100 µl 35% PCA. Samples were subsequently neutralized with 55 µl 7M KOH. Glucose, pyruvate, lactate, formate, acetate, succinate and ethanol contents were determined by HPLC (LKB) with a REZEX organic acid analysis column (Phenomenex) at 45ºC with 7.2 mM H_2SO_4 as eluent, using an RI 1530 refractive index detector (Jasco) and AZUR chromatography software for data integration.

Determination of in vivo P/O

During full anaerobic growth, ATP is produced only by substrate-level phosphorylation. Therefore, the $q_{ATP}^{fermentation}$ can be calculated from the net production of ATP, which under these conditions is equal to the sum of ethanol and acetate production minus glycerol production, as the production of glycerol from glucose in anaerobic conditions costs one ATP per glycerol formed:

$$q_{ATP}^{fermentation} = q_{Ethanol} + q_{Acetate} - q_{Glycerol} \qquad \text{(Equation 1)}$$

It follows from $\mu = q \cdot Y$ that if the yield on ATP is identical in anaerobic and aerobic cultivations of otherwise identical chemostat, the specific rate of ATP production (q_{ATP}) is also identical. Therefore;

$$q_{ATPtotal}^{\ anaerobic} = q_{ATPtotal}^{\ aerobic} = q_{ATPtotal}^{\ micro-aerobic} \qquad \text{(Equation 2)}$$

When the cells have a respiro-fermentative metabolism in glucose-limited chemostats, both substrate level phosphorylation (in the cytosol) and mitochondrial oxidative phosphorylation contribute to ATP generation. Therefore,

$$q_{ATPtotal}^{\ respiro-fermentative} = q_{ATP}^{\ fermentation} + q_{ATP}^{\ respiration} \qquad \text{(Equation 3)}$$

The total ATP synthesis during respiration is covered by the activity of the ATP synthases, which is dependent on the oxygen flux and the P/O. In addition, substrate level phosphorylation by glycolytic and TCA cycle activity, which yields ATP, has to be included. Converting glucose into two acetyl-CoA yields two ATP molecules and two CO_2 molecules. In the TCA cycle two molecules of ATP and four CO_2 are formed. Concluding, per glucose molecule four ATP molecules and six CO_2 molecules are formed. Since in full glucose oxidation ($C_6H_{12}O_6$ + 6 O_2 → 6 CO_2 + 6 H_2O) CO_2 production is equal to O_2 consumption, the q_{ATP} from substrate level phosphorylation equals $^2/_3$ q_{O2}. Therefore, the total ATP flux from respiration equals;

$$q_{ATP}^{\ respiration} = 2P/O \cdot q_{O_2} + \frac{2}{3} q_{O_2} \qquad \text{(Equation 4)}$$

Which means that $q_{ATPtotal}$ equals;

$$q_{ATPtotal} = q_{Ethanol} + q_{Acetate} - q_{Glycerol} + (2P/O \cdot q_{O_2}) + \frac{2}{3} q_{O_2} \qquad \text{(Equation 5)}$$

The $q_{ATPtotal}$ is determined in anaerobic cultures otherwise identical to the aerobic cultivations. After determination of $q_{Ethanol}$, q_{O2}, q_{CO2}, $q_{Acetate}$ and $q_{Glycerol}$ in normal aerobic cultures, we calculated respiratory efficiency as;

$$P/O = \frac{q_{ATPtotal} - q_{Ethanol} - q_{Acetate} + q_{Glycerol} - \frac{2}{3} q_{O_2}}{2 q_{O_2}} \qquad \text{(Equation 6)}$$

Electron microscopy

To study the morphology of the mitochondria 10 ml of broth was quickly quenched in 10 ml pre-heated 4% paraformaldehyde, 0.4% glutaraldehyde in 0.1 M phosphate buffer pH 7.0 and incubated for 15 minutes at the cultivation temperature. Cells were washed in 2% paraformaldehyde, 0.2% glutaraldehyde in 0.1 M phosphate buffer pH 7.0 and incubated for 1 hour at room temperature on a rocking plate. Cells were stored in 1% paraformaldehyde in

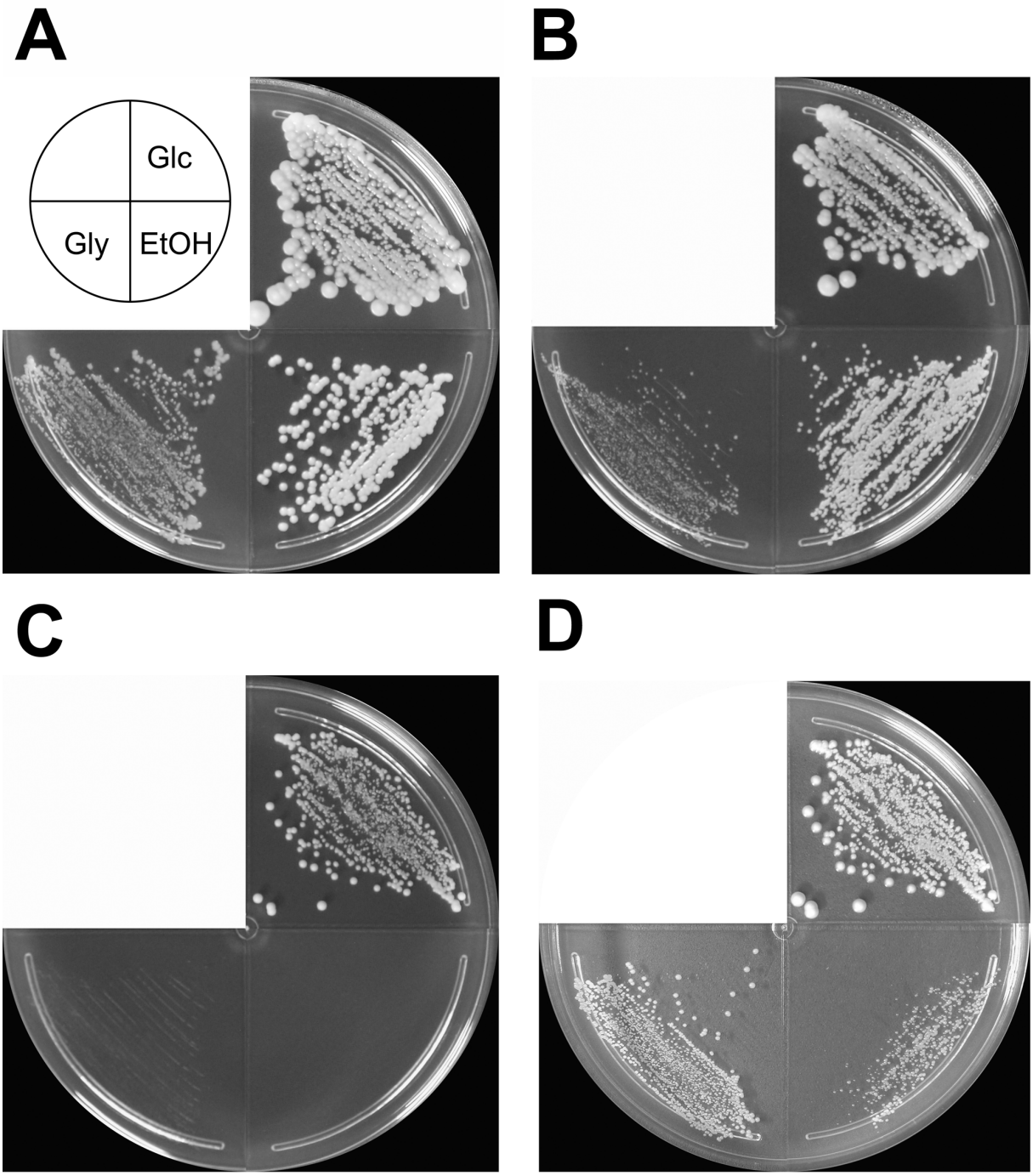

Figure 4.2. The effect of incubation temperature on wild-type cells grown on YP plates with different carbon sources. Plates were incubated for 24 hours at *A.* 30ºC *B.* 37ºC and *C.* 38ºC. *D.* Plates incubated at 38ºC for 24 hours, and subsequently at room temperature for 48 hours.

1.0 M phosphate buffer at 4ºC. Thereafter, the yeast cells were three times rinsed with distilled water, and subsequently postfixed in freshly prepared 2% potassium permanganate for 45 minutes. After rinsing with distilled water the yeast cells were dehydrated in an increasing series of ethanol (50%, 70%, 80%, 90%, 95% and three times 100%), infiltrated with 25%, 50%, 70% and 100% Spurr's resin (Low viscosity embedding media Spurr's kit, EMS), and finally embedded in freshly prepared Spurr's resin and polymerized at 70ºC. After

ultramicrotomy, the 90 nm sectioned yeast cells were post-stained with 4% uranylacetate/distilled water for 20 minutes and after rinsing with distilled water with 0.4% leadcitrate for 4 minutes. The yeast cells were viewed with a Tecnai 12 electron microscope (FEI, the Netherlands) at 80 kV.

RESULTS

Yeast respiratory growth is temperature sensitive

In our previous studies, we observed a switch from respiratory to respiro-fermentative metabolism when we cultured yeast in glucose limited chemostats at temperatures above 37ºC [3]. We therefore decided to test if yeast respiratory growth is affected by temperature on carbon sources that yield energy only through respiratory metabolism. We cultivated yeast on plates containing glucose, glycerol or ethanol as the sole carbon source, and incubated the plates at different temperatures. Indeed, although growth was observed on all three carbon sources at 30ºC and 37ºC (Figure 4.2A and 4.2B), yeast completely failed to grow at 38ºC on glycerol or ethanol (Figure 4.2C). Incubation of the same plates at room temperature after the 38ºC cultivation revealed that the imposed growth arrest was reversible, and that the cells had retained the capability of respiratory growth at permissive temperatures (Figure 4.2D). This suggests that mitochondrial respiratory function at higher temperature is insufficient to sustain growth and that the function can be recovered by culturing at lower temperatures.

To study the effect of temperature on mitochondrial functioning thoroughly, we used carbon-limited chemostats with a dilution rate of 0.1 h^{-1} and glucose as the only carbon and energy source. From these cultures the overall steady state carbon fluxes were analyzed (Table 4.2A). We observed fully respiratory metabolism from 30ºC to 37ºC. Ethanol production was observed at cultivation temperatures higher than 37ºC. Interestingly, the specific oxygen consumption rate was constant at all temperatures, even those above 37ºC. Since the biomass yield on ATP (Y_{ATP}) is suggested to decrease upon an increase in temperature [7, 26], we expected an increase in the glycolytic flux with increasing temperature. However, glycolytic fluxes and yield on glucose were not changed in the range of 30ºC-37ºC (Table 4.2A). This suggests that either the Y_{ATP} does not decrease with increasing temperatures, or that the ATP production per glucose molecule is increased.

Yeast respiratory chain efficiency increases with increasing temperature

In order to understand the contributions of respiration and fermentation to the energy required for growth, we developed a method to determine the efficiency of the respiratory chain *in vivo*. The efficiency of the respiratory chain is defined as the P/O, the production of ATP per oxygen consumed. This value expresses the efficiency of the respiratory chain

Table 4.2. *A.* Physiological data of wild type baker's yeast in glucose limited aerobic chemostats cultivated at various temperatures. *B.* Physiological data of wild type baker's yeast in glucose limited anaerobic chemostats cultivated at various temperatures. *C.* Physiological data of wild type baker's yeast in glucose limited chemostats cultivated at various concentrations oxygen in the input gas at 30ºC.Values represent the mean ± standard deviation of data obtained from at least three independent steady-state chemostat cultures.

A

Culture temperature	DW	$q_{Glucose}$	q_{O2}	q_{CO2}	$q_{Ethanol}$	$q_{Glycerol}$	Yield	Carbon recovery
	g/l	mmol gDW^{-1} h^{-1}					g/g	%
30ºC	3.8 ± 0.1	1.1 ± 0.1	2.9 ± 0.3	2.9 ± 0.3	0.0 ± 0.0	0.0 ± 0.0	0.5 ± 0.0	104 ± 5
34ºC	3.7 ± 0.1	1.1 ± 0.0	2.7 ± 0.1	2.7 ± 0.0	0.0 ± 0.0	0.0 ± 0.0	0.5 ± 0.0	99 ± 3
37ºC	4.0 ± 0.1	1.1 ± 0.0	2.6 ± 0.2	2.6 ± 0.1	0.0 ± 0.0	0.0 ± 0.0	0.5 ± 0.0	97 ± 2
38ºC	0.6 ± 0.1	7.2 ± 0.8	3.0 ± 0.6	13 ± 1.4	9.7 ± 1.7	0.6 ± 0.4	0.1 ± 0.0	92 ± 6

B

Culture temperature	DW	$q_{Glucose}$	q_{CO2}	$q_{Acetate}$	$q_{Ethanol}$	$q_{Glycerol}$	Yield	Carbon recovery
	g/l	mmol gDW^{-1} h^{-1}					g/g	%
30ºC	0.8 ± 0.1	5.3 ± 0.4	9.4 ± 0.0	0.2 ± 0.0	6.4 ± 0.1	0.7 ± 0.1	0.1 ± 0.0	94 ± 3.0
34ºC	0.8 ± 0.1	6.0 ± 0.2	10 ± 3.0	0.0 ± 0.0	9.0 ± 0.5	1.1 ± 0.1	0.1 ± 0.0	93 ± 5.6
37ºC	0.7 ± 0.1	6.0 ± 0.1	8.3 ± 0.7	0.0 ± 0.0	11 ± 0.6	1.3 ± 0.1	0.1 ± 0.0	96 ± 4.1
38ºC	0.6 ± 0.1	6.7 ± 0.1	13 ± 2.5	0.0 ± 0.0	11 ± 0.4	1.2 ± 0.1	0.1 ± 0.0	95 ± 4.6

C

% O_2 input	DW	$q_{Glucose}$	q_{O2}	q_{CO2}	$q_{Acetate}$	$q_{Ethanol}$	$q_{Glycerol}$	Carbon recovery
	g/l	mmol gDW^{-1} h^{-1}						%
0.00	0.8 ± 0.1	5.3 ± 0.0	0.0 ± 0.0	9.4 ± 0.0	0.2 ± 0.0	6.4 ± 0.1	0.7 ± 0.0	94 ± 3.0
0.41	1.2 ± 0.0	3.6 ± 0.1	0.9 ± 0.0	6.7 ± 0.1	0.0 ± 0.0	5.3 ± 0.1	0.0 ± 0.0	99 ± 2.6
0.83	1.4 ± 0.1	3.2 ± 0.1	1.7 ± 0.0	7.3 ± 0.1	0.0 ± 0.0	3.9 ± 0.2	0.0 ± 0.0	98 ± 3.6
1.80	2.4 ± 0.1	1.8 ± 0.0	2.1 ± 0.1	3.9 ± 0.1	0.0 ± 0.0	0.9 ± 0.0	0.0 ± 0.0	91 ± 0.5
2.25	2.9 ± 0.2	1.4 ± 0.0	2.3 ± 0.0	3.3 ± 0.1	0.0 ± 0.0	0.3 ± 0.0	0.0 ± 0.0	95 ± 3.1
3.35	3.0 ± 0.0	1.4 ± 0.1	2.4 ± 0.0	3.3 ± 0.0	0.0 ± 0.0	0.3 ± 0.0	0.0 ± 0.0	94 ± 2.8
20.95	3.8 ± 0.1	1.1 ± 0.1	2.9 ± 0.3	2.9 ± 0.3	0.0 ± 0.0	0.0 ± 0.0	0.0 ± 0.0	104 ± 5

when measured in isolated mitochondria. In literature a constant P/O is often assumed, for instance to calculate the ATP flux [30]. We, however, determined the P/O by determining *in vivo* ATP fluxes in combination with oxygen consumption fluxes. Growth yields in aerobic organisms depend on both the Y_{ATP} and the P/O. Therefore, Y_{ATP} and the P/O cannot be determined independently in aerobic cultures. We decided to determine Y_{ATP} in anaerobic continuous culture, where fermentation is the only ATP generating pathway. We assume that the Y_{ATP} is similar in aerobic and anaerobic conditions, which is valid for *E. coli* [24, 31]. Therefore, we can use the ATP production rate determined in anaerobic cultures to calculate the P/O in aerobic cultivations (see Materials and Methods).

To determine the temperature dependence of the respiratory efficiency we measured the temperature dependence of ethanol flux, and thus q_{ATP}, in anaerobic chemostats (Table 4.2B). Figure 4.3 shows a linear correlation between $q_{ATPtotal}$ and temperature in the range from 30ºC to 38ºC under anaerobic conditions. This indicates that the ATP demand increased with increasing cultivation temperature, even up to temperatures at which the cells could no longer grow on respiratory carbon sources (Figure 4.2). Using this q_{ATP}, we determined P/O in aerobic conditions, comparing aerobic chemostats to anaerobic chemostats at the same temperature. Remarkably, in the range of 30ºC to 37ºC the P/O increased from 0.7 to 1.4 (Figure 4.3). However, a further increase of the culture temperature to 38ºC led to a steep decrease of the P/O ratio to a point where the oxygen consumption is no longer coupled to ATP production, as the *in vivo* P/O was zero (Figure 4.3).

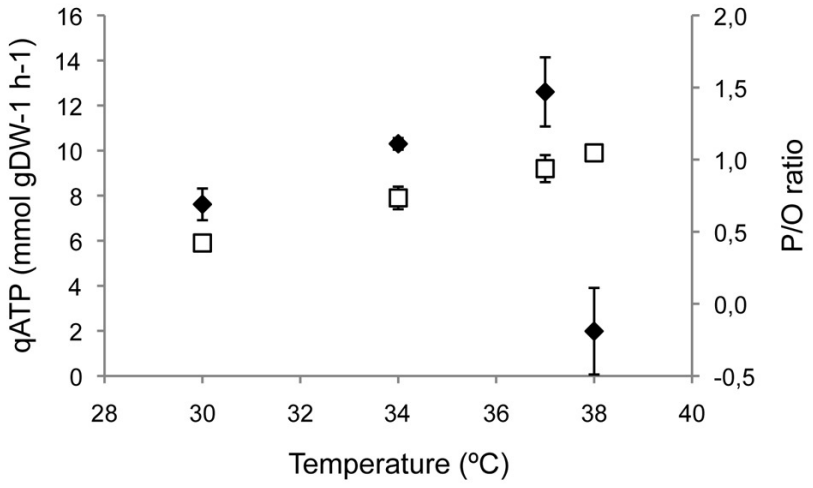

Figure 4.3. Temperature dependence of q_{ATP} (open squares) and P/O (solid diamonds) in wild-type steady-state cultivations.

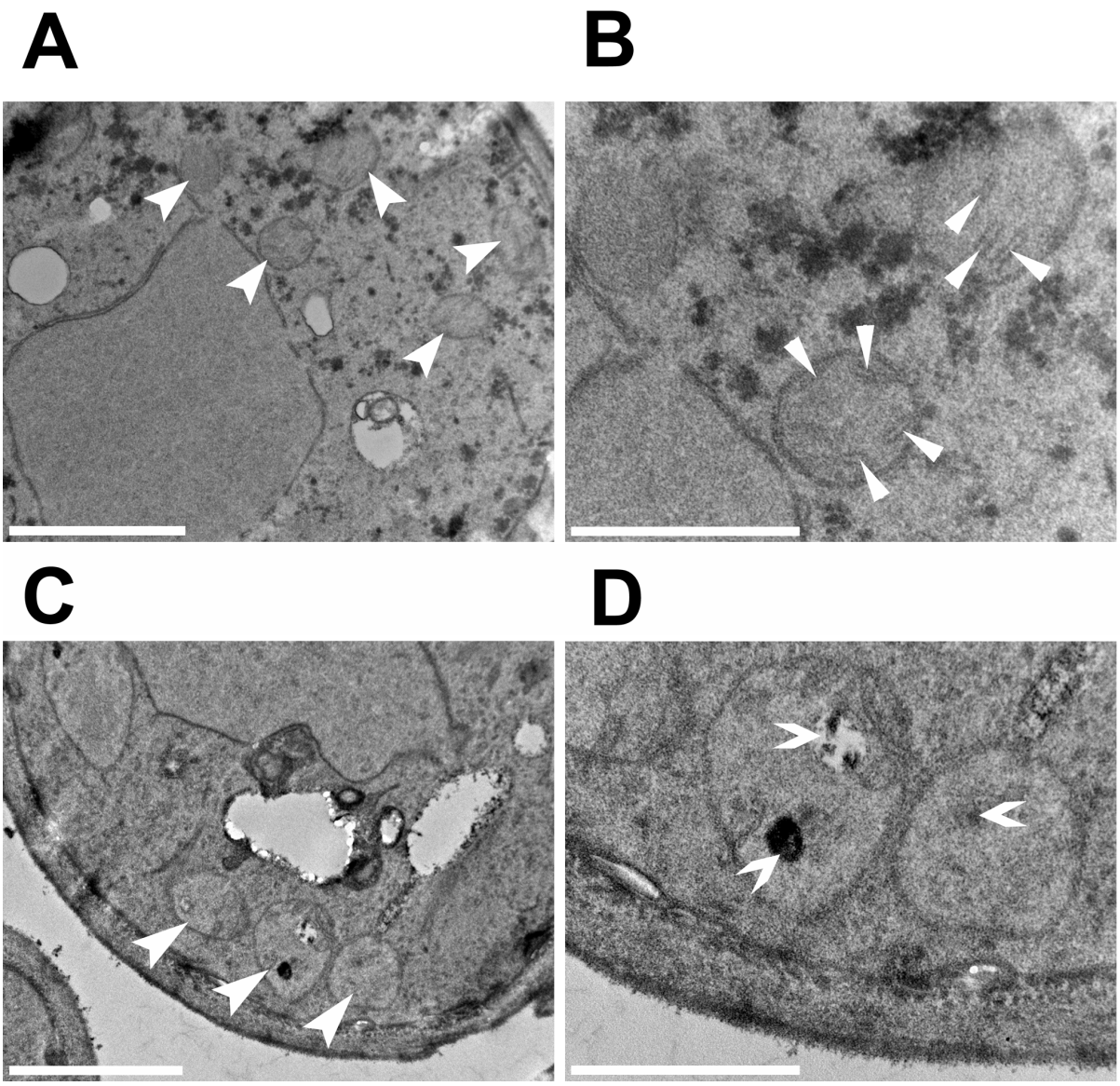

Figure 4.4. Electron micrographs of representative cells cultivated at 30ºC (*A,B*) and 38ºC (*C,D*). In panels *A* and *C*, arrowheads indicate mitochondria. Filled arrowheads in panel *B* indicate cristae, while v-shaped arrowheads in panel *D* indicate dense bodies inside mitochondria. Size bars in the left panels correspond to 1µm in the right panels to 500 nm.

Alteration of mitochondrial inner membrane structure by high temperature

The defect in mitochondrial respiratory chain mediated energy generation at 38ºC can: (i) be a rapid phenomenon, indicating a metabolic or transcriptionally regulated process; (ii) a direct effect of temperature on membrane structure, or a slow process, caused by accumulating damage; or (iii) inefficient mitochondrial biogenesis and thus requiring several generations to establish. Temperature shift experiments in which chemostats cultivations were shifted from 30ºC to 38ºC, or vice versa, indicated that the metabolic fluxes in either case were stable during the first 24 hours after the shift before gradually changing to those expected for a steady state at the new temperature (data not shown). This suggests that at the observe

effects are not due to a direct biophysical effect of the high temperature, or a metabolic or transcriptionally regulated uncoupling of the respiratory chain, but rather to defects in mitochondrial biogenesis, inheritance, or damage repair. We analyzed cellular mitochondrial content and morphology in samples from steady state cultures at both temperatures using fluorescence microscopy with MitoTracker, a dye that passively diffuses across the plasma membrane and accumulates in active mitochondria by the membrane potential [32]. No differences in the number of mitochondria or intensity of the mitochondrial staining could be observed (data not shown). However, a more detailed analysis using transmission electron microscopy revealed that the structure of the mitochondrial inner membranes was severely affected by cultivation at 38ºC; mitochondria of cells grown at 30ºC all show cristae (Figure 4.4A and B), whereas in cells cultivated at 38ºC increased slightly in diameter, had no clear cristae and contained electron dense bodies (Figure 4.4C and D).

Table 4.3. *A.* Physiological data of *gut2Δ* in glucose limited aerobic chemostats cultivated at various temperatures. *B.* Physiological data of *gut2Δ* in glucose limited anaerobic chemostats cultivated at various temperatures.

Values represent the mean ± standard deviation of data obtained from at least three independent steady-state chemostat cultures.

A

Culture temperature	DW	$q_{Glucose}$	q_{O2}	q_{CO2}	$q_{Ethanol}$	$q_{Glycerol}$	Yield	Carbon recovery
	g/l	mmol gDW^{-1} h^{-1}					g/g	%
30ºC	4.0 ± 0.3	1.1 ± 0.0	2.7 ± 0.2	2.7 ± 0.2	0.0 ± 0.0	0.0 ± 0.0	0.5 ± 0.0	106 ± 2
34ºC	3.7 ± 0.1	1.2 ± 0.1	3.2 ± 0.2	3.1 ± 0.2	0.0 ± 0.0	0.0 ± 0.0	0.5 ± 0.0	102 ± 4
37ºC	3.2 ± 0.3	1.3 ± 0.2	3.9 ± 0.3	3.8 ± 0.1	0.0 ± 0.0	0.1 ± 0.0	0.4 ± 0.1	105 ± 9

B

Culture temperature	DW	$q_{Glucose}$	q_{O2}	q_{CO2}	$q_{Ethanol}$	$q_{Glycerol}$	Yield	Carbon recovery
	g/l	mmol gDW^{-1} h^{-1}					g/g	%
30ºC	0.8 ± 0.0	4.9 ± 0.1	0.0 ± 0.0	6.8 ± 0.4	7.7 ± 0.6	0.9 ± 0.0	0.1 ± 0.0	95 ± 4
34ºC	0.7 ± 0.1	6.0 ± 0.2	0.0 ± 0.0	9.8 ± 0.3	8.6 ± 0.3	1.2 ± 0.2	0.1 ± 0.0	90 ± 1
37ºC	0.7 ± 0.0	7.1 ± 0.3	0.0 ± 0.0	11 ± 2.4	10 ± 1.0	1.3 ± 0.1	0.1 ± 0.0	89 ± 2

Temperature dependent regulation of respiratory chain efficiency depends on Gut2p

An increase in cultivation temperature from 30ºC-37ºC resulted in an increased respiratory chain efficiency. This strongly suggests regulation of the respiratory activity and ATP production in accordance to the ATP demand of the culture under different conditions. Yeast has no proton translocating complex I, but NADH dehydrogenases on the inside and outside of the mitochondrial inner membrane (Ndi1p, and Nde1p and Nde2p, respectively) [33, 34]. These accept the electrons from NADH and donate them to the ubiquinone pool [35]. Additionally, electrons from cytosolic NADH can be used by glycerolphosphate dehydrogenase, which converts DHAP into G3P. The latter is re-oxidized to DHAP via the FAD-dependent glycerol-3-phosphate dehydrogenase (Gut2p) in the intermembrane space [36] (Figure 4.1). The 2 electrons are donated to the mitochondrial ubiquinone pool to allow for oxygen reduction and ATP generation by the respiratory chain.

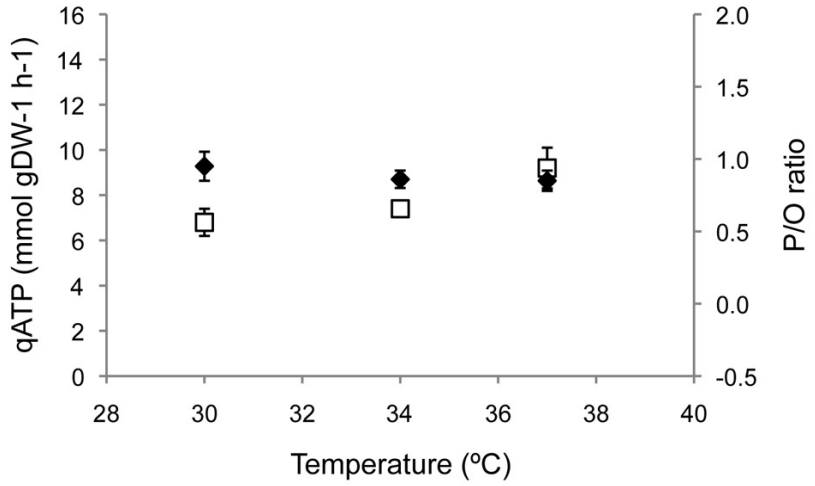

Figure 4.5. Temperature dependence of q_{ATP} (open squares) and P/O (solid diamonds) in *gut2Δ* steady-state cultivations.

Interestingly, *in vitro* data suggest that the G3P-shuttle is more efficient than the NADH dehydrogenases, with a measured a P/O of 1.7 when isolated mitochondria were supplied with G3P as a substrate, versus a P/O of 1.2 when NADH was used as a substrate [37]. We therefore hypothesized that the observed increase in respiratory efficiency at higher cultivation temperatures might be caused by a larger contribution of the G3P shuttle. To test this hypothesis, we determined ATP production rates and P/O at various temperatures in a strain deleted for *GUT2*. The deletion strain was cultivated in glucose-limited chemostat cultivations at a dilution rate of 0.1 h^{-1} at various temperatures. From these cultivations the overall steady state fluxes were calculated (Table 4.3A). In the range of 30ºC-37ºC the cultures showed a full respiratory metabolism. As expected from the studies with wild type

cells, the metabolism changed for cultivation temperatures higher than 37ºC leading to ethanol production. Table 4.3B shows the physiological data of the *gut2* deletion mutant in glucose-limited anaerobic chemostats. The q_{ATP} increased linearly with an increase in temperature and is comparable to the q_{ATP} determined in wild-type cultivations (Figure 4.2B). We used these data to calculate the P/O at a specific temperature for the deletion strain. Figure 4.5 shows that in contrast to the WT, in which the P/O showed a linear increase from 0.7-1.4, in the *gut2* deletion strain the P/O remained constant in the range of 30ºC-37ºC at a value of ~0.9. This implies that the increased efficiency observed in wild-type cultures depends on an enhanced contribution of the G3P shuttle.

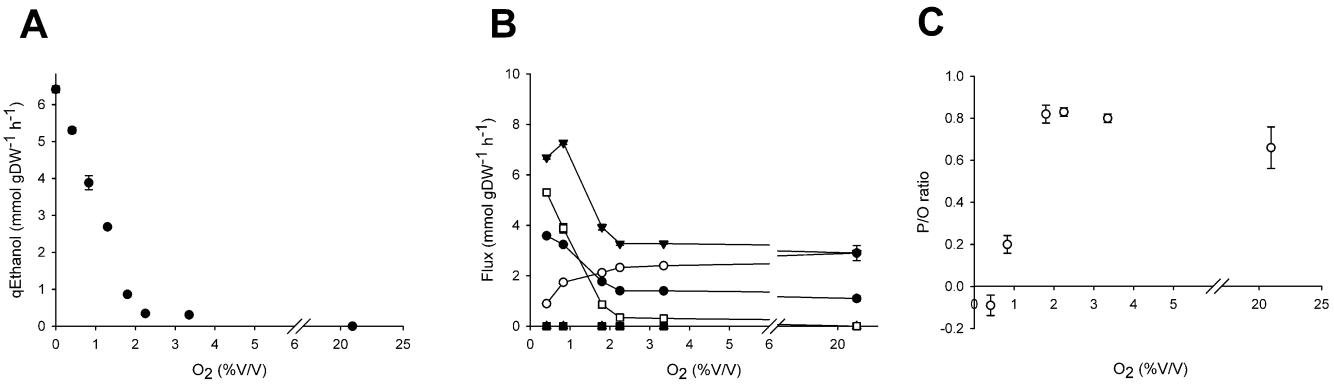

Figure 4.6. The effect of oxygen availability on physiological characteristics of glucose limited aerobic chemostat cultures grown at 30ºC. *A.* The effect of oxygen availability on steady-state ethanol production. *B.* The effect of oxygen level in the input gas on glucose flux (solid circles), oxygen flux (open circles), carbon dioxide flux (solid triangles), acetate flux (solid squares) and ethanol flux (open squares). *C.* P/O at various oxygen levels.

Mitochondrial respiratory chain efficiency is reduced at low oxygen availability

To further study the regulation of respiratory chain efficiency, we assessed the effect of oxygen availability. We hypothesized that under lowered oxygen partial pressure, the efficiency of the respiratory chain with respect to the oxygen consumption should be optimized in order to sustain high yield on glucose and growth. To study the efficiency of the respiratory chain in relation to oxygen availability we quantitatively determined the physiologically relevant range of oxygen concentrations. In *E. coli,* oxygen availability is inversely correlated with the production of acetate [31]. In yeast, not acetate but ethanol is the main fermentation product. We studied the relation of ethanol production rate with oxygen supply. Wild type yeast was cultivated with various supply rates of oxygen in chemostats with glucose as only carbon and energy source at a dilution rate of 0.1 h^{-1}. Overall steady-state fluxes were analyzed for product formation rates and glucose and oxygen consumption rates. Like the acetate production in *E. coli*, we established an inverse

linear relation with the production of ethanol in relation to the supply of oxygen in *S. cerevisiae* (Figure 4.6A). The minimal concentration of oxygen in the input gas for fully respiratory metabolism was determined at 2%. Between 2% and 21% oxygen in the input gas, only very minor changes in ethanol flux were observed. Below 2% oxygen in the input gas an increase in ethanol concentration was observed, indicating a shift to respiro-fermentative metabolism.

In this range of oxygen concentrations, we determined the respiratory chain efficiency. Overall steady-state fluxes were calculated (Table 4.2C and Figure 4.6B) and q_{ATP} and P/O were determined as outlined above. Figure 4.6C shows a P/O of around 0.8 for oxygen concentrations down to 1.80%. Below this concentration, lowering of the oxygen availability induced a decrease of the P/O from 0.8 to zero at 0.41% oxygen (Figure 4.6C), indicating that under these conditions respiratory chain activity did not contribute to ATP synthesis.

DISCUSSION

In order to survive and adapt to environmental changes, cells change their internal composition to one suitable for growth at the new conditions. Adaptive responses can put a significant additional energetic burden on the cells. A way to challenge the increased maintenance energy without affecting growth is to shift to a metabolism strategy that yields most energy and to maximize the efficiency of the existing mechanisms. Complete oxidation of glucose to carbon dioxide yields most ATP per glucose. Therefore energy generation via mitochondrial respiratory chain is a logic strategy when the maintenance energy is increased. We determined a P/O of around 0.8 in cells grown at 30ºC, which is lower than the theoretically maximal P/O of 1.3-1.5 when cells are growing in full respiratory conditions (Table 4.4). The efficiency of the respiratory chain can be affected at multiple levels: (i) at the level of coupling between the electron and proton fluxes (redox slip); (ii) at the level of proton leaks across the mitochondrial inner membrane; and (iii) at the level of coupling between proton flux and ATP synthesis by the ATP synthases.

Table 4.4. Theoretical *in vivo* and measured *in vitro* respiratory chain efficiencies

NADH reduction	P/O without scalars	P/O with scalars	*In vitro* P/O
Ndi	1.38	1.50	
Nde	1.38	1.27	1.2*
Gut2	1.38	1.38	1.7*
Ndo	0.69	0.58	0.6**

* Data from Larsson *et al.* [37]

** Data from De Santis and Melandri [44]

We observed a linear increase in efficiency of the respiratory chain in cultures grown in the temperature range of 30ºC-37ºC, which was caused by the increased contribution of the G3P-shuttle. It remains unclear how the increased contribution of Gut2p results in an increased efficiency. At all temperatures electrons are introduced into the RC at the ubiquinone pool, to which the same number of electrons is transferred per NADH molecule oxidized. Since *S. cerevisiae* lacks a classical proton translocating complex I [35] the same number of protons can be translocated for either of these routes of entry. Surprisingly, when Gut2p oxidizes cytosolic glycerol 3P the P/O is much higher. This difference in efficiency might be caused by redox slippage or proton leaks at 30ºC, which are reduced with the increase in temperature. Alternatively, a more efficient electron transfer to ubiquinone or the coupling of protons to the ATP synthases might occur at increased temperatures. It is thought that the mitochondrial NADH dehydrogenases are associated in a supramolecular complex [38] and therefore functionally interact with each other and might have competition for electron transfer. Indeed, electrons coming from Nde1p take precedence over electrons coming from Ndi1p or Gut2p [39], but whether the actual electron transfer is more or less efficient is unknown. One final factor may be the local consumption of protons in the NADH reduction itself, which takes place on the matrix face of the inner membrane (Ndi1p), the IMS face of the inner membrane (Nde1,2p) or in the cytosol (Gut2p). Theoretically, this proton consumption may alter the proton motive force, and create differences in the effective P/O for the three systems (see Table 4.4).

Limitation of the oxygen availability leads to a reduced respiratory flux. Since the respiratory flux and efficiency appear to be correlated [40-42], a decrease in oxygen availability should therefore increase the efficiency. We studied the effect of various oxygen concentrations in the input gas on the respiratory efficiency. At fully aerobic conditions the efficiency of the mitochondria, reflected by the P/O, was 0.7 (Figure 4.6C). Decreasing the oxygen input to 1.80% oxygen in the input gas did not result in a significant change in respiratory efficiency (Figure4. 6C). A further reduction of the oxygen input resulted in a steep decline of efficiency. Proton slip in cytochrome C oxidase has been reported to be of physiological relevance. By this slip the reduction of oxygen to water can be increased to prevent excessive electronegativity of respiratory carriers, which may explain the phenomenon. However, cytochrome c oxidase has a very high affinity for oxygen so that the respiratory chain can function at low oxygen tensions [43]. Alternatively or additionally, a distinct NADH dehydrogenase system with a lower efficiency might be induced at lower oxygen levels. In a yeast mutant blocked in ubiquinone synthesis, NADH oxidation was observed which was insensitive to Antimycin A, which blocks transfer of electrons to complex III, but was sensitive to KCN, blocking O_2 reduction, suggesting the existence of such a dehydrogenase [44]. Electrons would be donated directly to cytochrome c, and therefore no

protons translocation occurs at complex III, but only at complex IV (Figure 4.1, Table 4.4). Such a system might explain the initial decrease in P/O, but would not explain the full uncoupling.

Our initial observation was a lack of growth on respiratory carbon sources. Indeed, temperatures above 37ºC resulted in a strong decrease of the respiratory chain efficiency, with a P/O close to zero (Figure 4.3). Therefore, at 38ºC ATP synthesis was facilitated by fermentation alone, even while oxygen consumption rates were not decreased. The consumed oxygen might be used in processes other than at complex IV in the respiratory chain. However, it has previously been shown that these anabolic oxygen fluxes only represent a few percent of the total oxygen flux in normal conditions [45] (and references therein), and they are therefore unlikely to justify the entire oxygen consumption at 38ºC.

An explanation for the collapse in efficiency might be accumulated mitochondrial damage, or defects in mitochondrial generation of inheritance. Electron microscopy revealed mitochondria with fewer cristae, often in combination with the appearance of electron dense bodies in the matrix in cells grown at 38ºC (Figure 4.4), which might indicate that the mitochondria have lost structural integrity. Disintegration of cristae and dense bodies in the matrix has been observed in mammalian cells treated with ethidium bromide [46]. Ethidium bromide is thought to inhibit mitochondrial RNA synthesis and suppress mitochondrial protein synthesis [47-49]. Besides, mitochondrial DNA does not encode all components of the respiratory chain [50-52], and therefore mutants defective in mitochondrial DNA, rho^0 cells, have incomplete assembly of oxidative phosphorylation machinery. This has impact on the mitochondrial structures; mitochondria of rho^0 mutants have disorganized cristae and are greatly reduced in number [53]. If mitochondrial protein import is blocked, mitochondria likely end up like rho^0 mutants, with incomplete respiratory machinery. Mge1p, the nucleotide exchange factor for mHsp70p, essential for mitochondrial protein import was shown to exhibit reversible conformational change and dimer dissociation at temperatures above 37ºC [54]. This is not sufficient to explain the phenomenon observed, as overexpression of Mge1p did not suppress the respiratory growth deficiency at high temperature (data not shown), but similar mechanism might be functional.

Alternatively, internal damage may have an effect on mitochondrial functioning. It has been described that overexpression of antioxidants increases the maximal respiratory temperature [55]. Antioxidants neutralize ROS and therefore prevent cellular damage. The increased levels of antioxidants by overexpression may neutralize increased ROS production in the mitochondria at higher temperatures. Therefore, under these conditions, cells can respire at temperatures higher than they normally do. In our case, it might be that at 38ºC ROS induced damage is slowly accumulating. In time, the increased damage might result in

the loss of coupling of the respiratory chain to the ATP synthesis or the loss of translocation of protons.

Our study revealed highly dynamic respiratory chain efficiency, induced by variation in growth conditions. Cultivations at increased temperatures (30ºC-37ºC) showed an increase in respiratory efficiency and increasing the temperature even further (38ºC) resulted in loss of coupling of the respiratory chain and the ATP synthases. We have shown that the increased P/O was due to an increased flux through the G3P pathway, since in Gut2p deletion strain no increase in respiratory chain efficiency was observed. Under micro-aerobic conditions, where oxygen availability is challenged, the efficiency of mitochondrial respiration decreased. Switching to a previously described alternative NADH-dehydrogenase [44], which is directly coupled to the cytochrome c oxidase via cytochrome c, may contribute to this decrease. We must conclude that we still do not understand the full width of the regulation of central carbon metabolism in yeast, studied for such a long time. A full understanding is relevant for fermentation industry, but also for proper insight into apoptosis and ageing, as mitochondrial function and respiratory chain ROS production are central aspects of these phenomena.

ACKNOWLEDGEMENTS

The authors thank Jose Kiewiet and Nadja Schmidt for technical assistance and the members of the IOP consortium for stimulating discussions. For funding we thank SenterNovem, IOP Genomics Initiative, Project IGE3006A (JP, IT) and the Netherlands Organisation for Scientific Research (NWO), SYSMO-LAB project (MB).

REFERENCES

1. Bouwman, J., et al., *Metabolic regulation rather than de novo enzyme synthesis dominates the osmo-adaptation of yeast.* Yeast, 2011. **28**(1): p. 43-53
2. Gasch, A.P. and M. Werner-Washburne, *The genomics of yeast responses to environmental stress and starvation.* Funct Integr Genomics, 2002. **2**(4-5): p. 181-92.
3. Postmus, J., et al., *Quantitative Analysis of the High Temperature-induced Glycolytic Flux Increase in Saccharomyces cerevisiae Reveals Dominant Metabolic Regulation.* J Biol Chem, 2008. **283**(35): p. 23524-32.
4. Smits, G.J. and S. Brul, *Stress tolerance in fungi -- to kill a spoilage yeast.* Curr Opin Biotechnol, 2005. **16**(2): p. 225-30.
5. Strassburg, K., et al., *Dynamic transcriptional and metabolic responses in yeast adapting to temperature stress.* OMICS, 2010. **14**(3): p. 249-59.
6. Tempest, D.W. and O.M. Neijssel, *The status of YATP and maintenance energy as biologically interpretable phenomena.* Annu Rev Microbiol, 1984. **38**: p. 459-86.
7. Verduyn, C., *Physiology of yeasts in relation to biomass yields.* Antonie Van Leeuwenhoek, 1991. **60**(3-4): p. 325-53.
8. Warner, J.R., *The economics of ribosome biosynthesis in yeast.* Trends Biochem Sci, 1999. **24**(11): p. 437-40.
9. Pirt, S.J., *The maintenance energy of bacteria in growing cultures.* Proc R Soc Lond B Biol Sci, 1965. **163**(991): p. 224-31.
10. Pronk, J.T., H. Yde Steensma, and J.P. Van Dijken, *Pyruvate metabolism in Saccharomyces cerevisiae.* Yeast, 1996. **12**(16): p. 1607-33.
11. Brookes, P.S., *Mitochondrial H(+) leak and ROS generation: an odd couple.* Free Radic Biol Med, 2005. **38**(1): p. 12-23.
12. Brown, G.C., *The leaks and slips of bioenergetic membranes.* Faseb J, 1992. **6**(11): p. 2961-5.
13. Boveris, A. and B. Chance, *The mitochondrial generation of hydrogen peroxide. General properties and effect of hyperbaric oxygen.* Biochem J, 1973. **134**(3): p. 707-16.
14. Turrens, J.F. and A. Boveris, *Generation of superoxide anion by the NADH dehydrogenase of bovine heart mitochondria.* Biochem J, 1980. **191**(2): p. 421-7.
15. Nicholls, D.G. and R.M. Locke, *Thermogenic mechanisms in brown fat.* Physiol Rev, 1984. **64**(1): p. 1-64.
16. Rolfe, D.F. and M.D. Brand, *The physiological significance of mitochondrial proton leak in animal cells and tissues.* Biosci Rep, 1997. **17**(1): p. 9-16.
17. Juszczuk, I.M. and A.M. Rychter, *Alternative oxidase in higher plants.* Acta Biochim Pol, 2003. **50**(4): p. 1257-71.
18. Maxwell, D.P., Y. Wang, and L. McIntosh, *The alternative oxidase lowers mitochondrial reactive oxygen production in plant cells.* Proc Natl Acad Sci U S A, 1999. **96**(14): p. 8271-6.
19. Berthold, D.A., M.E. Andersson, and P. Nordlund, *New insight into the structure and function of the alternative oxidase.* Biochim Biophys Acta, 2000. **1460**(2-3): p. 241-54.

20. Jarmuszkiewicz, W., et al., *First evidence and characterization of an uncoupling protein in fungi kingdom: CpUCP of Candida parapsilosis.* FEBS Lett, 2000. **467**(2-3): p. 145-9.
21. Luevano-Martinez, L.A., et al., *Identification of the mitochondrial carrier that provides Yarrowia lipolytica with a fatty acid-induced and nucleotide-sensitive uncoupling protein-like activity.* Biochim Biophys Acta, 2009.
22. Kerscher, S., et al., *Yarrowia lipolytica, a yeast genetic system to study mitochondrial complex I.* Biochim Biophys Acta, 2002. **1555**(1-3): p. 83-91.
23. Sluse, F.E. and W. Jarmuszkiewicz, *Uncoupling proteins outside the animal and plant kingdoms: functional and evolutionary aspects.* FEBS Lett, 2002. **510**(3): p. 117-20.
24. Bekker, M., et al., *Respiration of Escherichia coli can be fully uncoupled via the nonelectrogenic terminal cytochrome bd-II oxidase.* J Bacteriol, 2009. **191**(17): p. 5510-7.
25. Stuart, R.A., *Supercomplex organization of the oxidative phosphorylation enzymes in yeast mitochondria.* J Bioenerg Biomembr, 2008. **40**(5): p. 411-7.
26. Wallace, R.J. and W.H. Holms, *Maintenance coefficients and rates of turnover of cell material in Escherichia coli ML308 at different growth temperatures.* FEMS Microbiology Letters, 1986. **37**(3): p. 317-320.
27. Mensonides, F., *PhD Thesis, University of Amsterdam.* 2007.
28. Verduyn, C., et al., *Effect of benzoic acid on metabolic fluxes in yeasts: a continuous-culture study on the regulation of respiration and alcoholic fermentation.* Yeast, 1992. **8**(7): p. 501-17.
29. Longtine, M.S., et al., *Additional modules for versatile and economical PCR-based gene deletion and modification in Saccharomyces cerevisiae.* Yeast, 1998. **14**(10): p. 953-61.
30. Verduyn, C., et al., *A theoretical evaluation of growth yields of yeasts.* Antonie Van Leeuwenhoek, 1991. **59**(1): p. 49-63.
31. Alexeeva, S., K.J. Hellingwerf, and M.J. Teixeira de Mattos, *Quantitative assessment of oxygen availability: perceived aerobiosis and its effect on flux distribution in the respiratory chain of Escherichia coli.* J Bacteriol, 2002. **184**(5): p. 1402-6.
32. Poot, M., et al., *Analysis of mitochondrial morphology and function with novel fixable fluorescent stains.* J Histochem Cytochem, 1996. **44**(12): p. 1363-72.
33. de Vries, S. and C.A. Marres, *The mitochondrial respiratory chain of yeast. Structure and biosynthesis and the role in cellular metabolism.* Biochim Biophys Acta, 1987. **895**(3): p. 205-39.
34. von Jagow, G. and M. Klinkenberg, *Pathways of Hydrogen in Mitochondria of Saccharomyces carlsbergensis.* Eur J Biochem, 1970. **12**: p. 583-592.
35. Onishi, T., *Mechanism of electron transport and energy conservation in the site I region of the respiratory chain.* Biochim Biophys Acta, 1973. **301**(2): p. 105-28.
36. Ronnow, B. and M.C. Kielland-Brandt, *GUT2, a gene for mitochondrial glycerol 3-phosphate dehydrogenase of Saccharomyces cerevisiae.* Yeast, 1993. **9**(10): p. 1121-30.
37. Larsson, C., et al., *The importance of the glycerol 3-phosphate shuttle during aerobic growth of Saccharomyces cerevisiae.* Yeast, 1998. **14**(4): p. 347-57.

38. Grandier-Vazeille, X., et al., *Yeast mitochondrial dehydrogenases are associated in a supramolecular complex.* Biochemistry, 2001. **40**(33): p. 9758-69.
39. Bunoust, O., et al., *Competition of electrons to enter the respiratory chain: a new regulatory mechanism of oxidative metabolism in Saccharomyces cerevisiae.* J Biol Chem, 2005. **280**(5): p. 3407-13.
40. Ouhabi, R., M. Rigoulet, and B. Guerin, *Flux-yield dependence of oxidative phosphorylation at constant [Delta]H+.* FEBS Lett, 1989. **254**(1-2): p. 199-202.
41. Fitton, V., et al., *Mechanistic stoichiometry of yeast mitochondrial oxidative phosphorylation.* Biochemistry, 1994. **33**(32): p. 9692-8.
42. Rigoulet, M., et al., *Quantitative analysis of some mechanisms affecting the yield of oxidative phosphorylation: dependence upon both fluxes and forces.* Mol Cell Biochem, 1998. **184**(1-2): p. 35-52.
43. Papa, S., F. Guerrieri, and N. Capitanio, *A possible role of slips in cytochrome C oxidase in the antioxygen defense system of the cell.* Biosci Rep, 1997. **17**(1): p. 23-31.
44. De Santis, A. and B.A. Melandri, *The oxidation of external NADH by an intermembrane electron transfer in mitochondria from the ubiquinone-deficient mutant E3-24 of Saccharomyces cerevisiae.* Arch Biochem Biophys, 1984. **232**(1): p. 354-65.
45. Rosenfeld, E. and B. Beauvoit, *Role of the non-respiratory pathways in the utilization of molecular oxygen by Saccharomyces cerevisiae.* Yeast, 2003. **20**(13): p. 1115-44.
46. McGill, M., T.C. Hsu, and B.R. Brinkley, *Electron-dense structures in mitochondria induced by short-term ethidium bromide treatment.* J Cell Biol, 1973. **59**(1): p. 260-5.
47. Lenk, R. and S. Penman, *Morphological Studies of Cells Grown in the Absence of Mitochondrial-Specific Protein Synthesis.* J Cell Biol, 1971. **49**(2): p. 541-546.
48. Perlman, S. and S. Penman, *Mitochondrial protein synthesis: resistance to emetine and response to RNA synthesis inhibitors.* Biochem Biophys Res Commun, 1970. **40**(4): p. 941-8.
49. Zylber, E. and S. Penman, *Mitochondrial-associated 4 S RNA synthesis inhibition by ethidium bromide.* J Mol Biol, 1969. **46**(1): p. 201-4.
50. Herrmann, J.M. and W. Neupert, *Protein transport into mitochondria.* Curr Opin Microbiol, 2000. **3**(2): p. 210-4.
51. Koehler, C.M., S. Merchant, and G. Schatz, *How membrane proteins travel across the mitochondrial intermembrane space.* Trends Biochem Sci, 1999. **24**(11): p. 428-32.
52. Pfanner, N. and A. Geissler, *Versatility of the mitochondrial protein import machinery.* Nat Rev Mol Cell Biol, 2001. **2**(5): p. 339-49.
53. Gilkerson, R.W., et al., *Mitochondrial DNA depletion causes morphological changes in the mitochondrial reticulum of cultured human cells.* FEBS Lett, 2000. **474**(1): p. 1-4.
54. Moro, F. and A. Muga, *Thermal adaptation of the yeast mitochondrial Hsp70 system is regulated by the reversible unfolding of its nucleotide exchange factor.* J Mol Biol, 2006. **358**(5): p. 1367-77.

55. Harris, N., et al., *Overexpressed Sod1p acts either to reduce or to increase the lifespans and stress resistance of yeast, depending on whether it is Cu(2+)-deficient or an active Cu,Zn-superoxide dismutase.* Aging Cell, 2005. **4**(1): p. 41-52.